Desalination and Water Treatment
www.deswater.com
doi: 10.5004/dwt.2021.27516

232 (2021) 187–197
August

Effective removal of diazinon and imidacloprid toxins from aqueous samples by nano poly(4,4′-methylenedianiline)/graphene oxide

Ali Toolabi[a], Esmail Mohseni[b,*], Mohammad Reza Zare[c], Nezamaddin Mengelizadeh[b], Elham Rostami[d], Mahmoud Taghavig[e], Sam Kharazi[f]

[a]*Department of Environmental Health Engineering, School of Public Health, Bam University of Medical Sciences, Bam, Iran, P.O. Box: 76169-13555, email: atoolabi@yahoo.com*
[b]*Department of Chemistry, Faculty of Science, University of Zanjan, Zanjan, Iran, 45371-38791, Tel. +98-917-781-1596; emails: Mohseniesmail@yahoo.com (E. Mohseni), Nezammengli65@gmail.com (N. Mengelizadeh)*
[c]*Research Center of Health, Safety and Environment, Department of Environmental Health Engineering, School of Evaz Health, Larestan University of Medical Sciences, Larestan, Iran, P.O. Box: 74318-95639, email: Zaremohammad1363@yahoo.com*
[d]*Department of Chemistry, Faculty of Science, University of Ahvaz, P.O. Box: 61357-15794, Ahvaz, Iran, email: Elhamrostami74@gmail.com*
[e]*Department of Environmental Health, Social Determinants of Health Research Center, Gonabad University of Medical Sciences, Gonabad, Iran, P.O. Box: 96917-93718, email: Taghavi66@yahoo.com*
[f]*Department of Medicine, Bam Univercity of Medical Sciences, Bam, Iran, email: Hony.Kharazi20@gmail.com*

Received 10 November 2020; Accepted 27 May 2021

ABSTRACT

In the present research, sheet nano poly(4,4′-methylenedianiline)/graphene oxide (nPMDA/GO) adsorbent has been used to remove diazinon and imidacloprid, as high consumption pesticides, from aqueous solutions. nPMDA/GO has been synthesized by in situ electropolymerization method. Fourier-transform infrared spectroscopy, field-emission scanning electron microscopy techniques, thermal gravimetric analysis, differential thermal analysis and X-ray diffraction analyses have been employed to analyze physicochemical characteristics of produced adsorbent. The concentration of diazinon and imidacloprid in water was measured using high-performance liquid chromatography. In order to obtain an efficient adsorbent for sorption of diazinon and imidacloprid, various parameters related to the adsorption process such as deposition time, temperature, ionic strength, pH, concentration of the nPMDA/GO, and concentration of diazinon and imidacloprid were optimized. The maximum removal efficiencies of diazinon (72.17%) and imidacloprid (66.7%) by nPMDA/GO were obtained at pollutants concentrations of 25 mg L^{-1}, a low absorbent concentration of 0.12 g L^{-1} and, contact time of 120 min and alkali pH. The results indicate that the adsorption of studied pesticides was dependent on ionic strength. By increasing the ionic strength (adjusted by $CaCl_2$ concentration), the adsorption of herbicides can be significantly decreased. Equilibrium empirical data have been fitted by Langmuir and Freundlich isotherms. Correlation coefficients showed that equilibrium data were better matched with the Freundlich model for imidacloprid and Langmuir model for diazinon. Kinetic data have been fitted with pseudo-first-order and pseudo-second-order models; according to the obtained correlation coefficients. It can be stated that the pseudo-second-order model is more suited to the kinetic data related to pesticide adsorption on nPMDA/GO adsorbent.

Keywords: Diazinon; Imidacloprid; Graphene oxide; Adsorption; Nanocomposite

* Corresponding author.

1. Introduction

With the rapid growth of urbanization and industrialization of cities, the problem of pollutant emissions into the ecosystem, even at very low concentrations, has raised concern in many parts of the world [1]. Removal of metal pollutants and agricultural pesticides from water and wastewater has been the subject of stringent laws in many countries to control water pollution [2]. Therefore, in order to maintain the health of people, the environment, and the economic use of all available water resources, water pollution sources must be stopped and water quality improved. Agricultural poisons such as imidacloprid [3], diazinon [2], and oxadiazon [4] are among the most water pollutants. These organophosphorus and organochlorine pesticides have been released into the environment due to their use as war agents or agricultural pesticides [5]. The presence of these pollutants in the environment, in addition to the irreversible effects on the ecosystem and the creation of aesthetic dilemmas, have also adverse effects such as mutagenesis and cancer in living things [6]. Therefore, the removal of these compounds from the environment, especially drinking water, is of particular importance; so that the maximum limit set by the US Environmental Protection Agency (EPA) for most organophosphorus pesticides in drinking water is less than 30 μg L^{-1} [7]. The most common methods for the removal of toxins in water are chemical oxidation [8], electrochemical [9], chemical deposition, adsorption [10], biological removal [11], reverse osmosis [12,13], photocatalysis [14], and filtration [15]. One of the methods that have been of particular interest to researchers in recent years is the use of surface adsorption [16–19]. Adsorption methods are superior to other techniques due to their high efficiency, flexibility, design simplicity, low cost, easy performance, and minimal sludge production [20,21]. The main features of a good adsorbent are high capacity and fast adsorption [22,23]. These properties are obtained when the adsorbent has a high specific surface area and abundant surface adsorption sites. Among the adsorbents, graphene oxide nanoparticles have been used alone or in combination with other adsorbents to remove pollutants from aquatic environments due to their high potential, adsorption capacity, and high specific surface area [24,25]. The existence of hydrophilic oxygenated functional groups on the basal planes and edges of GO enables it to be functionalized through covalent and non-covalent bonds to yield versatile new materials [26]. So far, extensive industrial and academic research has been done to improve the properties and increase the applicability of graphene oxide nanoparticles in various fields. Keshvardoostchokami et al. [27] synthesized silver/graphene oxide nanocomposite and surveyed its usage in removal of imidacloprid from contaminated waters. Boruah et al. [28] reported Fe_3O_4/graphene oxide nanocomposite as an efficient adsorbent for triazine pesticides. In this regard, polymeric nanocomposites have a special place. Polymeric molecules such as diamines, aldehydes, polypropylenimine, iodobenzene and diisocyanate are suggested [29–31]. Koolivand et al. [26] used graphene oxide/polyimide nanocomposites as highly CO_2 selective membranes, which are effective for environmental problems. Mejias Carpio et al. [32] used graphene oxide functionalized with ethylenediaminetriacetic acid membrane to adsorb heavy metal [32]. Among the compounds, aniline monomers are special compounds due to their amine groups [33] which can enhance the properties of graphene oxide, in addition to removal of cationic and anionic contaminants from aqueous solutions [34–37]. 4,4′-methylenedianiline (MDA) is a derivative of aniline with primary amine (–NH_2) group substituted at the para-position [38]. The amine groups can enhance the properties of graphene oxide by connecting to the graphene surface through amide bond formation with a carboxyl group [39].

In this research, 4,4′-methylenedianiline/graphene oxide nanocomposite (nPMDA/GO) adsorbent was electrosynthesized using in situ method to absorb imidacloprid and diazinon from aqueous solutions. The effect of major factors such as contact time, initial pesticide concentration, adsorbent dosage, pH, and temperature was studied on the adsorption efficiency of pesticide. The kinetic and isotherm studies of the adsorption reactions were fully detailed and discussed.

2. Materials and methods

2.1. Chemicals and reagents

4,4′-methylenedianiline ($C_{13}H_{14}N_2$) functional monomer, lithium chloride (LiCl), and calcium chloride ($CaCl_2$) were purchased from Merck, (Germany). Diazinon (purity: 98.9%) and imidacloprid (purity: 98%) pesticides were purchased from Sigma-Aldrich, (Spain). The stock solution of diazinon and imidacloprid (1,000 mg L^{-1}) were prepared in deionized water. The graphite electrodes with the specifications given in Table 1 were prepared for in situ synthesis of the nanocomposite. All other chemicals were of analytical grade and commercially available and were used without further purification.

2.2. MDA-GO nanocomposite electrosynthesis

The electrosynthesis of nPMDA/GO composite was performed by an in situ electro-oxidation polymerization of MDA monomer in the presence of graphite electrodes. First, the graphite electrodes with a thickness of 3 mm and a distance of 3 cm were inserted into the reaction tube. Before use, the electrode surface was rinsed with water and ethanol solution. In a typical synthesis process, 5 mmol MDA monomer and 2 mmol lithium chloride electrolyte were added to 30 ml ethanol/water in the reaction tube. Electrosynthesis was done under ultrasonic conditions using an ultrasonic water bath

Table 1
Graphite compound

Compounds	Percentage
C	97%
Si	0.3%
Cu	0.4%
Mn	2.3%

(frequency 35 kHz mains connection 230 V) for 120 min. The polymerization reaction was initiated immediately after applying a potential difference of 6 V to the above solution. The precipitate was separated by centrifuge and after washing 3 times with distilled water and ethanol, and finally, was dried at room temperature.

2.3. Characterization

The concentration of diazinon and imidacloprid in solutions was measured using high-performance liquid chromatography (Agilent Technology 1260 Infinity series) with a C18 column (250 mm × 4.6 mm, 5 m). Water–methanol mixture (30:70 v/v) was used as a mobile phase at a flow rate of 1 ml min^{-1}. The limit of detection was found to be 0.03 and 0.07 ng μL^{-1} at selected wavelengths of 290 and 214 nm for diazinon and imidacloprid, respectively. The Fourier-transform infrared spectroscopy (FT-IR) was recorded using a Perkin Elmer Spectrum 65 device at 4,000–400 cm^{-1} from KBr pellets for the detection of functional groups. Thermal gravimetric analysis (TGA) was performed on STA BAHR 503 instrument in the temperature range of 5°C–550°C with a heating rate of 10°C min^{-1} under nitrogen atmosphere to evaluate the thermal stability of nPMDA/GO. The structure of adsorbents was investigated by recording X-ray diffraction (XRD) patterns with a SIEMENS D5000 X-Ray Diffractometer using Cu-Kα radiation (λ = 1.54059 Å) over the range of 10° < 2θ < 90°. FE-SEM images were taken by field-emission scanning electron microscopy (FE-SEM) on LEO 1455 VP equipped with an energy-dispersive X-ray (EDX) spectroscopy apparatus for analyzing the morphology of nanostructures and identifying chemical constituents.

2.4. Adsorption experiments

All adsorption experiments were performed in batch mode. The nPMDA/GO (30–150 mg) was added to 10 mL diazinon or imidacloprid solutions (25–400 mg L^{-1}) in 30 mL flasks, and they were agitated for 30–120 min at 200 rpm. The effect of other parameters including temperature (25–100) and initial pH (2–10) was also studied. Then, the mixture was filtered, and the treated samples were analyzed to estimate the pesticide adsorption capacity of the adsorbents. To investigate the particular effect of each parameter, one parameter was varied, while others were kept constant [40].

2.5. Adsorption isotherm

The adsorption isotherms designate the distribution of adsorbate between the liquid and solid phases in the equilibrium state. The adsorption equilibrium data were fitted using the Langmuir Eq. (1) and Freundlich Eq. (2):

$$\frac{C_e}{q_e} = \frac{1}{K_l q_m} + \frac{C_e}{q_m} \tag{1}$$

$$q_e = K_f C_e^{1/n} \tag{2}$$

where q_m is the maximum adsorption capacity (mg g^{-1}), K_l is the adsorption equilibrium constant (g mg^{-1}), characteristic of the affinity between the adsorbent and adsorbate. K_l and q_m can be obtained by linear regression of (C_e/q_e) vs. C_e data. Moreover, K_f is the Freundlich adsorption constant ((g $mg^{-1})^{1/n}$), which is an indicator of the adsorption capacity, while n refers to the adsorption tendency.

2.6. Adsorption kinetic

The mechanism of adsorption and the rate of the process can be investigated through important information provided by the kinetic study. The kinetic was studied based on the pseudo-second-order Eq. (3) and pseudo-first-order Eq. (4) model as follows:

$$\frac{t}{Q_t} = \frac{1}{kQ_e^2} + \frac{t}{Q_e} \tag{3}$$

$$\frac{t}{q_t} = \frac{1}{q_e^2 k_2} + \frac{1}{q_e} \tag{4}$$

where t is the adsorption time, Q_t is the amount of pesticides adsorbed at any time t, (mg g^{-1}), Q_e is the amount of pesticides saturated adsorbed (mg g^{-1}), k is the pseudo-second-order rate constant (g $(mg\ h)^{-1}$). The rate constant k can be obtained from the slope and the intercept of the plot of t/Q_t vs. t and where q_e (mg g^{-1}) is the adsorption capacity at equilibrium, q_t in (mg g^{-1}) is the adsorption capacity at a time t (min), k_2 (min^{-1}) is the pseudo-first-order rate constant.

3. Results and discussion

3.1. Characterization of nPMDA/GO

Fig. 1 shows the FT-IR spectrum for the nPMDA/GO nanocomposite. The abundance of functional groups with oxygen is a characteristic of GO. The wide and intense peaks at 3,400 cm^{-1} are related to the stretching vibration of OH, which indicates GO has a large amount of water molecules absorbed at the surface. Also clearly visible are the peaks at 1,017 cm^{-1}, which are related to the tensile vibration of the C–O–C bond, and the peaks at the 1,384 cm^{-1} represent the OH of the C–OH group. The peak of C=C group shows in the area of 1,615 cm^{-1} that it is related to graphene Sp^2 hybrid. The peak at 1,760 cm^{-1} belongs to the C–O group, which has operated and produced the carboxyl group (COOH). Clear peaks for MDA are seen at 2,900 and 2,850 cm^{-1}, which are related to the tensile vibration in the methylene group, and the peak at 3,373 cm^{-1}, which is related to the N–H bond. Strong absorption peaks of the quinonoid ring (C=N) appeared at 1,512 cm^{-1}. Amide group absorption peaks for nanocomposites have been observed at 1,620 cm^{-1}, which shows the amidation between GO carboxylic acid groups and amino groups in aniline. The interaction between GO and MDA is a combination of electrostatic interactions, hydrogen bonds, and π–π interactions (Fig. 2).

To evaluate the thermal properties of nPMDA/GO nanocomposite, TGA and differential thermal analysis (DTA) analyses were used in the temperature range of 25°C–550°C. Fig. 3 shows the TGA chart for nPMDA/GO. In nPMDA/GO nanocomposites, gradual weight loss to the temperature range of 100°C is caused by the loss

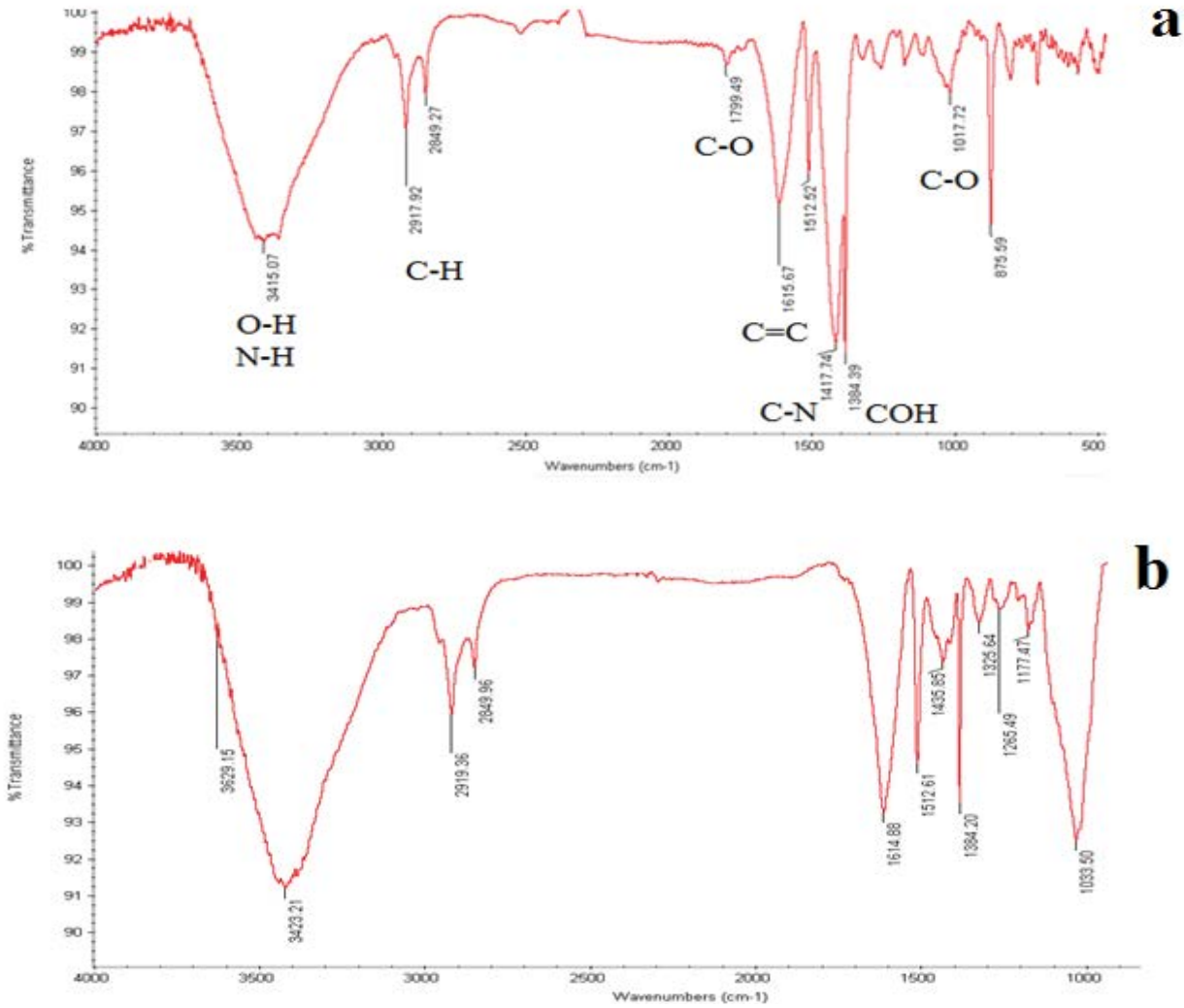

Fig. 1. FT-IR spectra of nPMDA/GO (a) and GO (b).

of moisture on the surface and between its layers. Then, at 100°C–300°C, the functional groups with oxygen in the GO are reduced from the nanocomposite structure. After a temperature of 300°C, MDA begins to break down into nanocomposite. Then, at temperatures above 450°C, the weight loss is related to the unstable carbon remaining in the structure and the decomposition of oxygen-containing groups such as ketones in the main structure to produce CO and CO_2. The DTG chart shows the two exothermic peaks which appear in the range of 270°C and 525°C, which approves TGA analysis. As a result, it can be said that nanocomposite has good thermal stability.

In order to study the structure of nPMDA/GO, the XRD spectrum of nanocomposite was taken (Fig. 4). As can be seen, the peak observed at an angle of 7.4° corresponds to the crystal plate of graphene oxide and shows that the graphene structure has not been degraded during the polymerization process and has been successfully placed on the MDA polymer. The peaks are also seen at angles 24.5° and 25.5°; these peaks are related to the scattering of graphene atoms, which is the flat surface of graphene formed between the layers of graphene surfaces. There are also peaks with angles of 17° and 21°, which are related to 4,4′-methylenedianiline.

FE-SEM images show the morphology and distribution of nanoparticles of graphene oxide. As shown in Fig. 5, graphene oxide is characterized by semi-transparent sheets with some particles and dimensions of 25 nanometer with small holes, which indicates the accuracy of the synthesized nPMDA/GO nanocomposite plates. In fact, the following analysis shows that the synthesized adsorbent has good porosity and can provide good adsorption capacity to adsorb contaminants. The EDX clearly showed the elementals of the nanocomposite (Fig. 6). The percentage compositions were 59.65%, 18.34% and 19.79% for carbon (C), nitrogen (N) and oxygen (O) in nPMDA/GO.

3.2. Removal studies

3.2.1. Mechanism of MB adsorption

When pesticides and nanocomposite adsorbent are mixed, the imine and hydroxide groups present on the

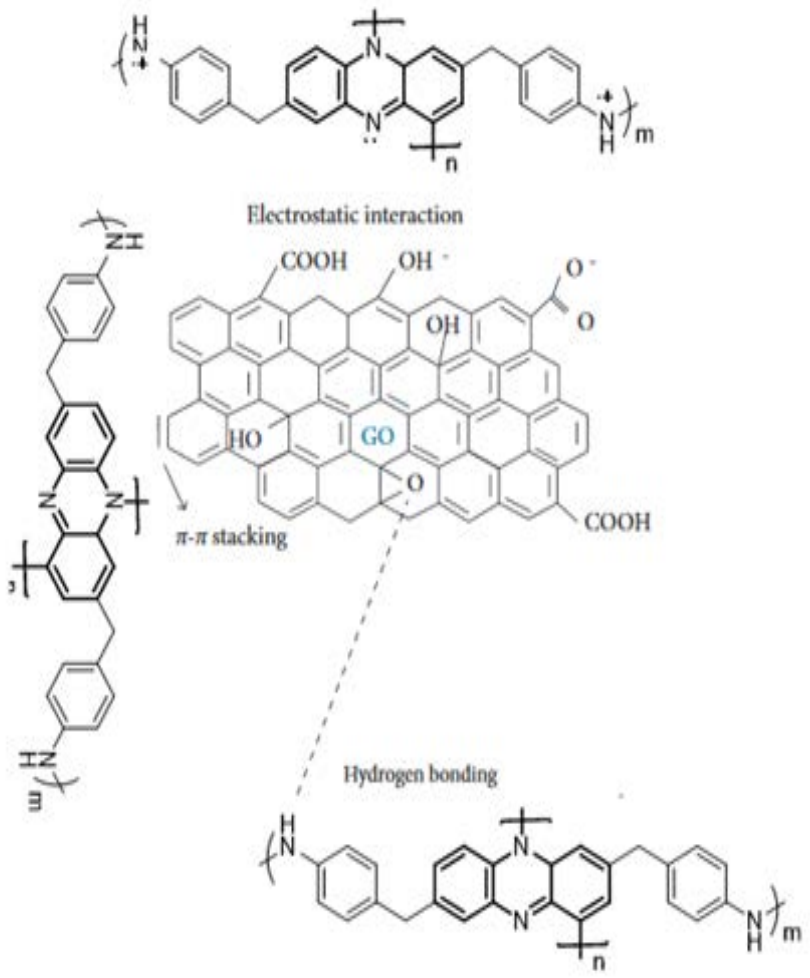

Fig. 2. Interaction between GO and MDA.

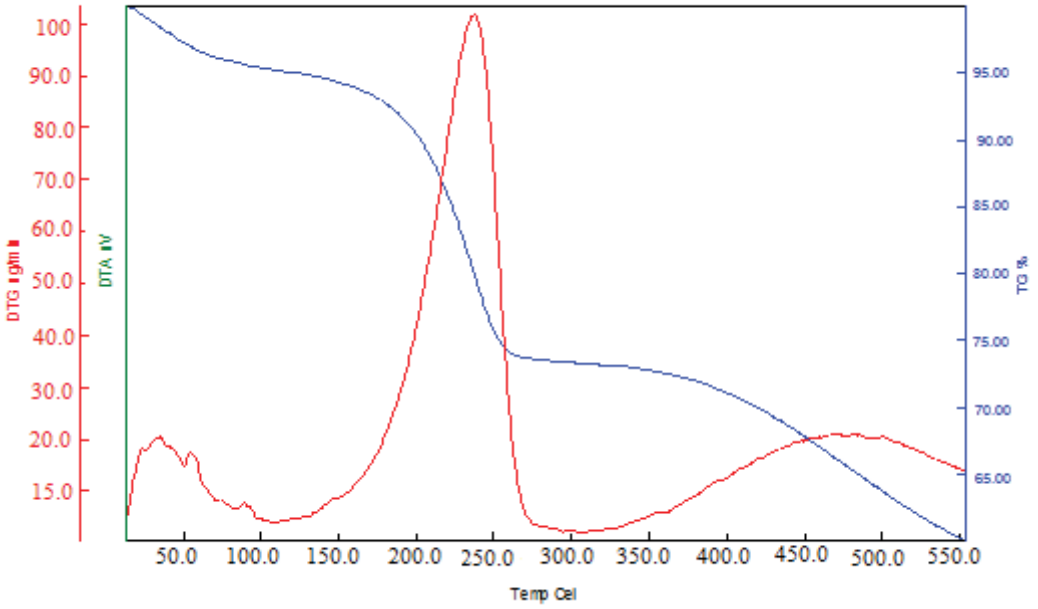

Fig. 3. TGA and DTA analysis of nPMDA/GO.

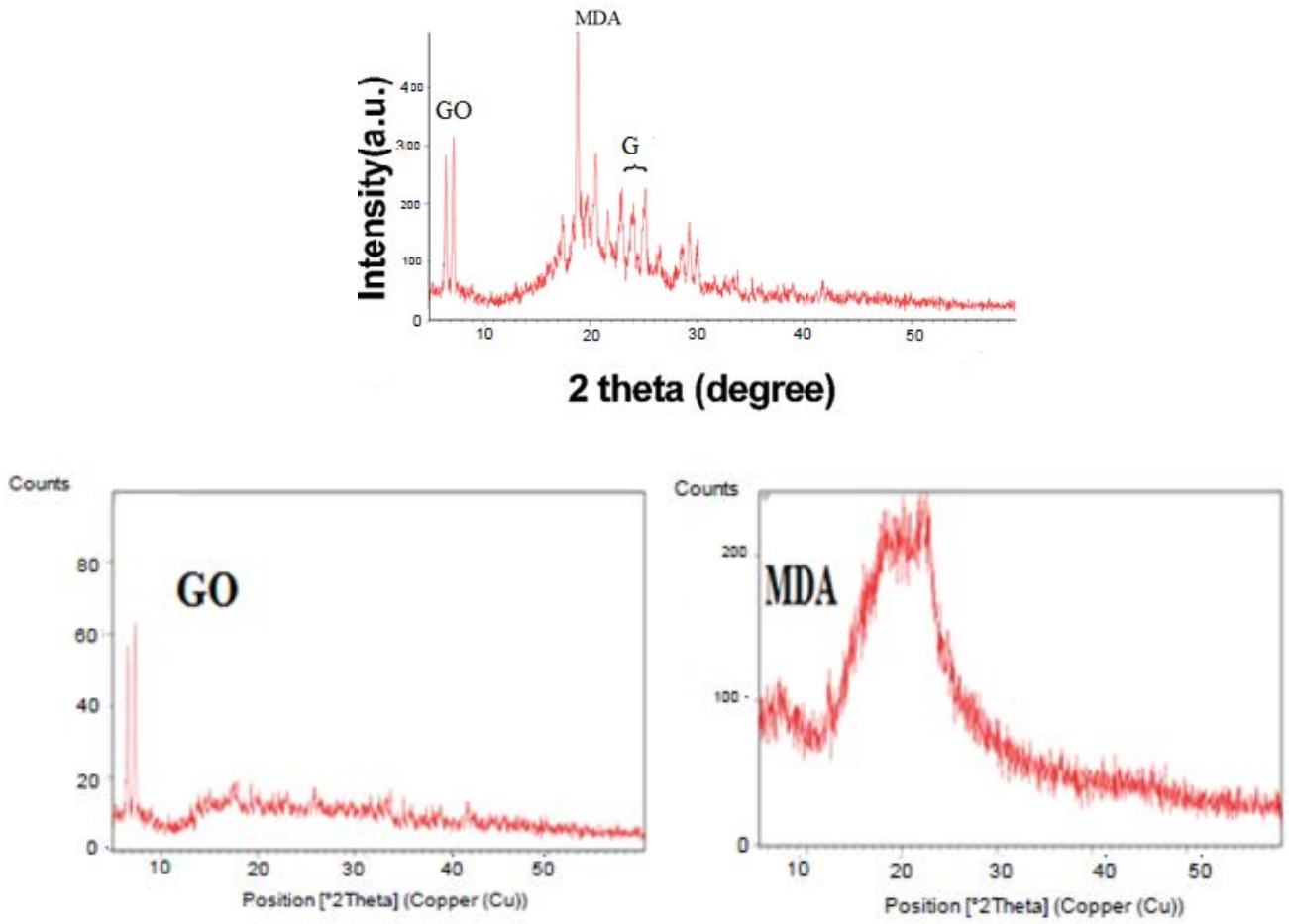

Fig. 4. XRD patterns of nPMDA/GO, GO, MDA.

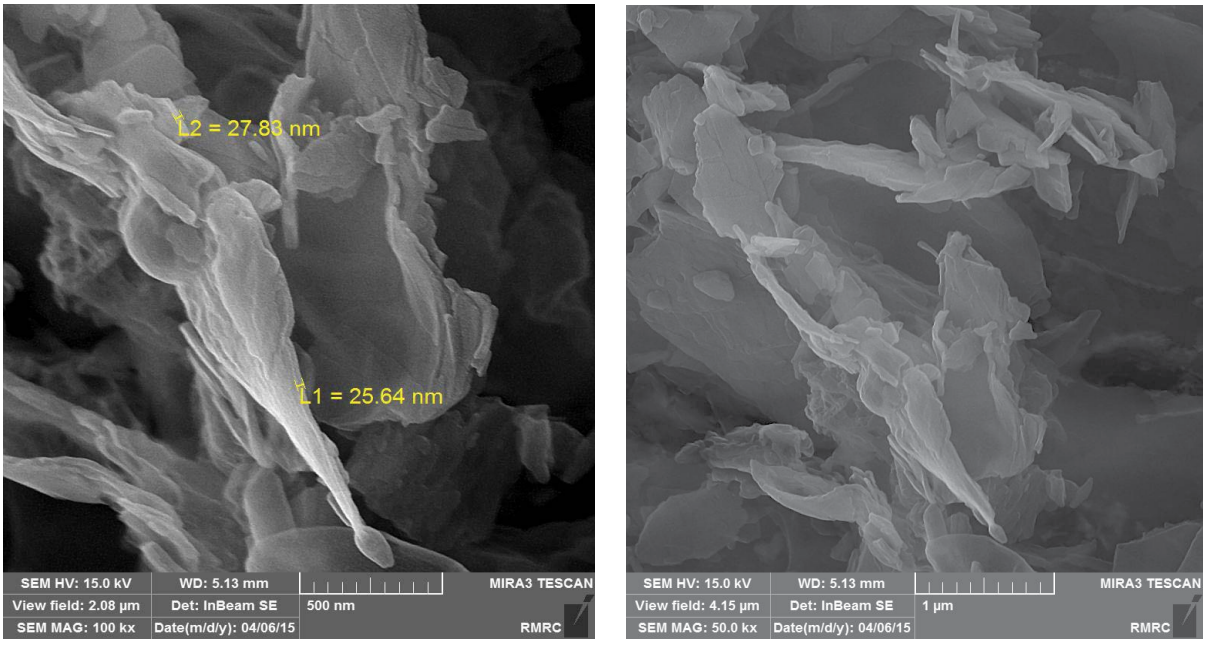

Fig. 5. FE-SEM images of nPMDA/GO.

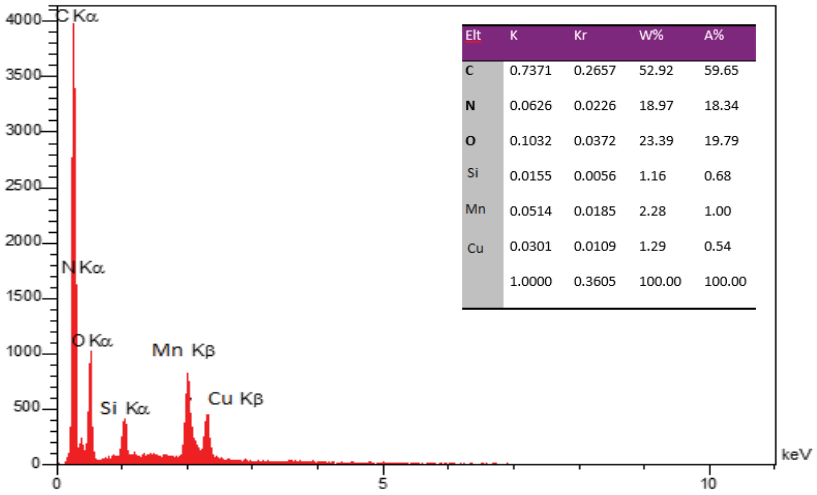

Elt	K	Kr	W%	A%
C	0.7371	0.2657	52.92	59.65
N	0.0626	0.0226	18.97	18.34
O	0.1032	0.0372	23.39	19.79
Si	0.0155	0.0056	1.16	0.68
Mn	0.0514	0.0185	2.28	1.00
Cu	0.0301	0.0109	1.29	0.54
	1.0000	0.3605	100.00	100.00

Fig. 6. EDX analysis of nPMDA/GO.

adsorbent surface form hydrogen bonding through reacting with functional groups of pesticides. In addition, due to the presence of aromatic rings in the adsorbent and pesticides, a π–π bond is formed between them, which these interactions lead to removing pesticides.

3.2.2. Effect of adsorbent dosage

In order to find the optimal amount of adsorbent that can absorb the highest amount of diazinon and imidacloprid contaminant, different amounts of nPMDA/GO were used and the elimination efficiency of toxins were monitored. Adsorbent dosage was varied in the range of 0.03–0.15 g, while all other parameters including temperature, agitation time, pH and shaking speed were constant. Fig. 7 shows that increasing the adsorbent dosage improves the removal percentage of pesticides, which the maximum removal of 66.67% for diazinon and 72.3% for imidacloprid was obtained at an adsorbent of 120 mg. It was found that, in the beginning, the adsorption mainly occurs on the surface of nPMDA/GO, so the adsorption rate is fast. After saturation of the surface adsorption, the adsorption gradually proceeds into the inner part of nPMDA/GO via the diffusion of pesticides into the nanocomposite matrix, which leads to a lower adsorption rate. By increasing the amount of adsorbent to 0.15 g, eliminating toxins does not significantly increase. Therefore, 0.12 g was selected as the most suitable dosage of adsorbent prepared in all removal experiments.

3.2.3. Effect of contact time

The deposition time of diazinon and imidacloprid contaminations removal from the solution was investigated for 120 min, the results of which are shown in Fig. 8. As can be seen, the absorption efficiency of diazinon and imidacloprid by nPMDA/GO nanocomposite is 73.12 and 69, respectively. In addition, the absorption equilibrium point was reached at about 120 min for adsorption. A significant increase in adsorption capacity at the beginning

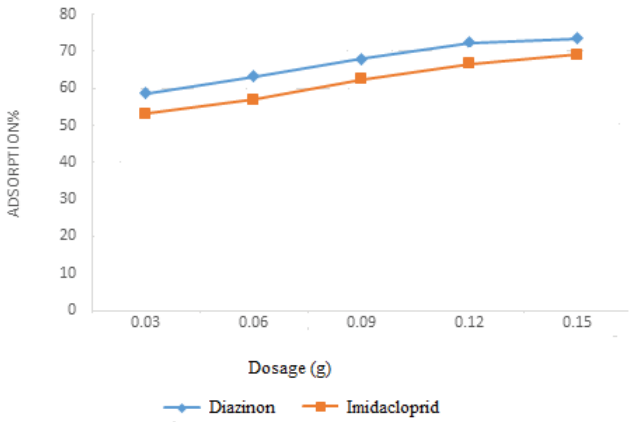

Fig. 7. Effect of adsorbent dose on the adsorption of imidacloprid and diazinon.

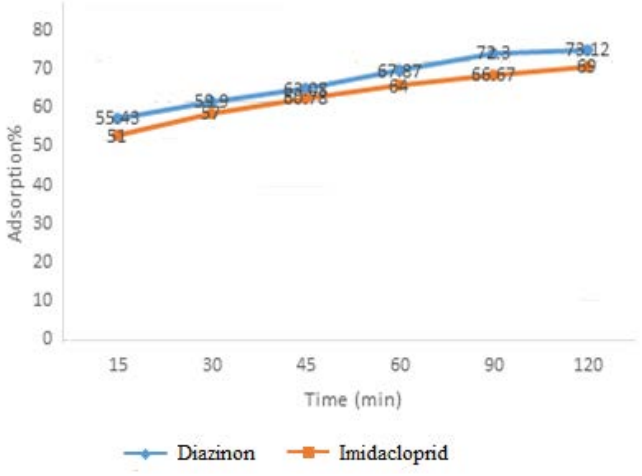

Fig. 8. Effect of contact time on the adsorption of imidacloprid and diazinon.

of the contact time can be due to the presence of high and unsaturated active sites of nMDA/GO adsorption level. Over time, this process slows down and stabilizes due to saturation of active sites, and the cavities are filled with adsorbate molecules. Similar findings have been reported by various researchers. Mushtaq et al. [41] evaluated effect of the contact time parameter on the removal of copper by using bentonite composite with *Eriobotrya japonica* seed adsorbent and showed that adsorption was initially fast and then decreased after a specific time and finally, reached the equilibrium.

3.2.4. Effect of pesticide concentration

To evaluate the adsorption performance of nPMDA/GO nanocomposite in presence of different concentrations of studied pesticides, its performance was investigated at diazinon and imidacloprid concentrations of 25 to 400 ppm while all other parameters were constant. As the initial concentration of toxins increases, the elimination percentage decreases and reaches its minimum at 400 ppm. At low primary concentration, vacant binding sites were available and percentage sorption was high, and when initial insecticide concentration was increased, the percentage sorption was reduced due to the saturation of binding sites on the adsorbent surface. Chang et al. [42], using activated carbon from rice straw agricultural waste for removal of carbofuran, indicated that when the initial pesticide concentration increased, the percentage removal decreased from 59% to 15%. As shown in Fig. 9, at higher concentrations, the adsorption process stops due to the saturation of the adorbent surface [43].

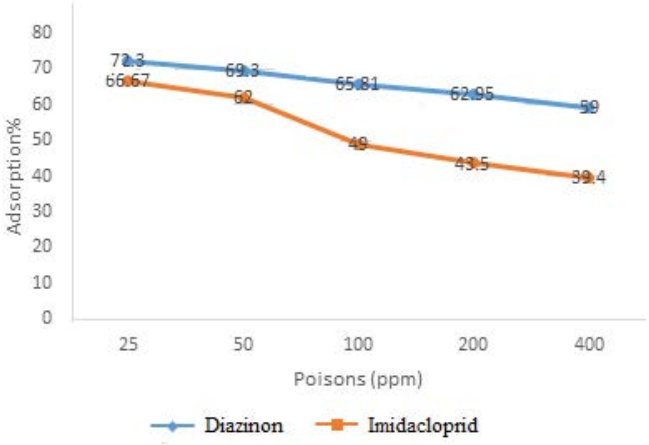

Fig. 9. Effect of initial concentration of imidacloprid and diazinon on the adsorption of imidacloprid and diazinon.

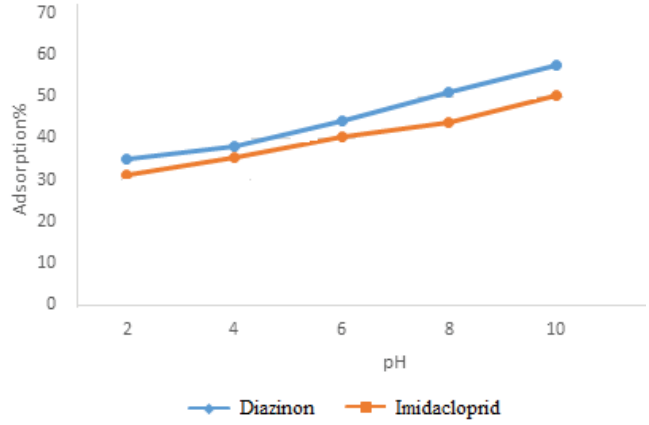

Fig. 10. Effect of pH on the adsorption of imidacloprid and diazinon.

3.2.5. Effect of pH

pH plays an important role in the adsorption efficiency of the nPMDA/GO. Functional groups available on the surface of nPMDA/GO such as amine and hydroxide groups are responsible for the sorption of diazinon and imidacloprid molecule because the structure of these surface functional groups was modified in different ways at different pH values. For this aim, pH of the adsorption media was varied in the range of 2–10, while other experimental conditions were remained the same (Fig. 10). Results clearly indicated that at lower pH values, there is a competition for the active sites between H^+ ions and pesticides molecule that reduced the adsorption efficiency. While in basic media, the competing effect of H^+ reduced and surface acquired negative charge, so the positively charged adsorbate molecules were attracted for adsorption. Fairooz et al. [44], using Pomegranate Peel for adsorption of pesticide, showed when pH increases, the electrostatic excretion between pesticides and surface sites decreases, and the pesticides sorption increases.

3.2.6. Effect of ionic strength

The effect of ionic strength on the adsorption of pesticides was shown in Fig. 11. The results show that the addition of Ca^{2+} ions decreased sorption. Two mechanisms may explain the decrease in adsorption of pesticides with increasing Ca^{2+} ion concentration. Firstly, Ca^{2+} ions can adsorb directly onto Functional groups available on the surface of nPMDA/GO and reducing its negative surface charge; this leads to reduce the electrostatic interaction between pesticides and adsorbent. Furthermore, the addition of divalent salt ($CaCl_2$) decreased the availability of the vacant sites on the adsorbent.

3.2.7. Effect of temperature

The sorption percentage of pesticides revealed a decreasing trend with increasing temperature (Fig. 12), which indicates that the adsorption is an exothermic process. This may be attributed to the fact that attractive forces between nPMDA/GO surface and pesticide are weakened and the sorption decreases [45]. In other words, rising temperature increases the kinetic energy and decreases the quantity of sorption. Moradi Kalhor et al. [3], by studying the removal of imidacloprid pesticide using silica nano hollow sphere (SNHS) and amino-functionalized silica nano hollow sphere (SNHS-NH2) adsorbents reported that as temperature rises, the adsorption rate is reduced.

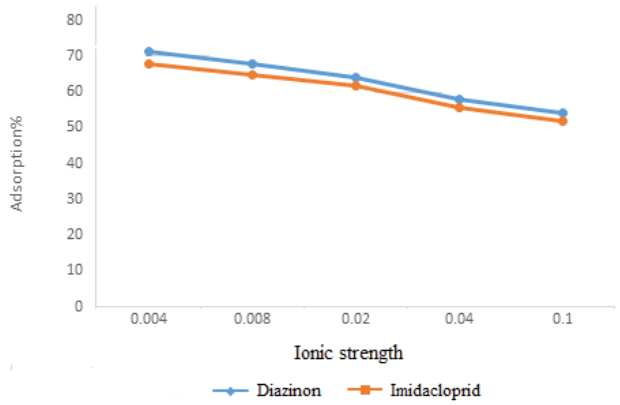

Fig. 11. Effect of ionic strength on the adsorption of imidacloprid and diazinon.

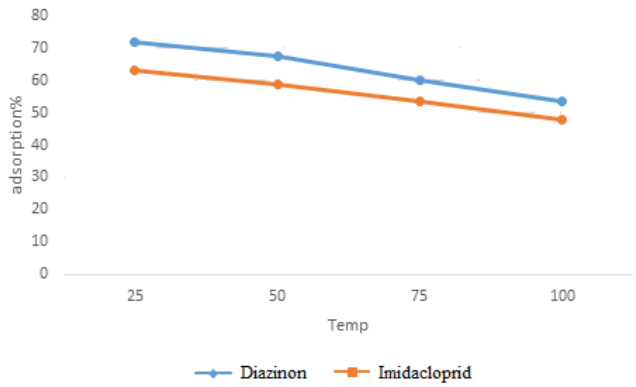

Fig. 12. Effect of temperature on the adsorption of imidacloprid and diazinon.

Table 2
Kinetic parameters for the adsorption of diazinon and imidacloprid onto nPMDA/GO adsorbent

Pseudo-second-order			Pseudo-first-order			Kinetic / Pesticide
q_e (mg g^{-1})	k_2 (min^{-1})	R^2	q_e (mg g^{-1})	k_1 (min^{-1})	R^2	
1.62	0.072	0.998	0.963	–0.001	0.921	Diazinon
1.52	0.082	0.999	0.960	–0.001	0.897	Imidacloprid

Table 3
Isotherms parameters for the adsorption of diazinon and imidacloprid onto nPMDA/GO adsorbent

Freundlich			Langmuir				Isotherms / Adsorbent
K_f (mg g^{-1})	N	R^2	R_L	q_{max} (mg g^{-1})	b (L mg^{-1})	R^2	
0.002	0.34	0.928	1.53	1.105	0.066	0.944	Diazinon
0.536	2.008	0.546	0.316	3.982	0.072	0.457	Imidacloprid

3.3. Kinetics study

Adsorption capacities of nPMDA/GO were tested as a function of time. All the adsorption rate constants and linear regression correlation coefficients are presented in Table 2. The data illustrate that the correlation coefficient pseudo-second-order model is more suitable to describe the adsorption kinetics process. Results specify that the rate-limiting step may be a chemical bonding in the adsorption process for pesticides. Similar kinetics trends have also been reported previously for different pollutants sorption onto composites such as rhodamine B dye on activated sludge [46].

3.4. Adsorption isotherms

The adsorption isotherms of nPMDA/GO for diazinon and imidacloprid were measured, and fitted by Langmuir and Freundlich models. As shown in Table 3, the Freundlich model can better represent the imidacloprid that it can be deduced the adsorption on a heterogeneous surface having binding sites with different energy contents. The Freundlich isotherm model is empirical in nature, which assumes that the stronger binding sites are occupied first, and binding strength decreases with increasing degree of site occupation [47]. Langmuir isotherm model better represents diazinon adsorption; based on this, it can be concluded that all the adsorption sites have the same energy level and adsorption occurs at specific homogeneous sites on the surface of the nPMDA/GO [48].

Table 4
Comparison of maximum adsorption capacity of adsorbents for diazinon and imidacloprid removal

Adsorbents	Sorption capacity	
	Diazinon	Imidacloprid
nPMDA/GO	72.17	66.7
nPMDA	53.01	46.78
GO	62.91	56.3

3.5. Efficiency comparison

To compare the sorption capacity of nMDA/GO with nPMDA and GO, their maximum adsorption capacities are reported in Table 4. Results indicated that the sorption capacity of nPMDA/GO was higher than that of other sorbents. It seems that multilayers structure and functional groups of nMDA/GO was the cause of this high sorption capacity (Nikzad et al. [20]).

4. Conclusion

The first step of this discussion was the preparation of the sheet nano 4,4′-methylenedianiline/graphene oxide by in situ electropolymerization method. The FT-IR, FE-SEM, and EDX techniques have been applied to identify the formed nanocomposite. FE-SEM images clearly indicate the nMDA/GO with different sizes, while the average particle diameter was in the range of 20–30 nm. The TGA and DTA analyses used to evaluate the thermal properties nMDA/GO. The result showed nanocomposite has good thermal stability up to 450°C. Also, the XRD spectrum of nanocomposite was taken to study the structure of nMDA/GO. The results showed that the nanocomposite has been successfully synthesized. Equilibrium tests have been conducted on diazinon and imidacloprid at different conditions. The results showed that the pesticide adsorption process is dependent on initial solution concentration, dosage amounts, adsorption temperature, and pH. The amounts of imidacloprid and diazinon were reduced at lower pH values for this system. In addition, the sorption percentage of pesticides was decreased by increasing the temperature. Pseudo-second-order kinetic model was found to be better fitted to the diazinon and imidacloprid adsorption data. The sorption isotherms were better fitted by the Freundlich for imidacloprid and Langmuir model for diazinon.

References

[1] H. Merrikhpour, M. Jalali, Comparative and competitive adsorption of cadmium, copper, nickel, and lead ions by Iranian natural zeolite, Clean Technol. Environ. Policy, 15 (2013) 303–316.
[2] S. Nikzad, A. Akbar Amooey, A. Alinejad-Mir, Adsorption of diazinon from aqueous solutions by magnetic guar gum-montmorillonite, Chem. Data Collect., 20 (2019) 100187, doi: 10.1016/j.cdc.2019.100187.
[3] M. Moradi Kalhor, A. Abbas Rafati, L. Rafati, A. Ali Rafati, Synthesis, characterization and adsorption studies of amino functionalized silica nano hollow sphere as an efficient adsorbent for removal of imidacloprid pesticide, J. Mol. Liq., 266 (2018) 453–459.
[4] M. Rahman, T.-H. Kim, G.-S. Kwon, J.E. Yang, M. Park, J.-E. Kim, Removal efficiency of the herbicide oxadiazon in treatment processes for drinking water, J. Korean Soc. Appl. Biol. Chem., 52 (2009) 252–257.
[5] M. Kazemi, A.M. Tahmasbi, R. Valizadeh, A.A. Naserian, A. Soni, Organophosphate pesticides: a general review, Agric. Sci. Res. J., 2 (2012) 512–522.
[6] M.B. Čolović, D.Z. Krstić, T.D. Lazarević-Pašti, A.M. Bondžić, V.M. Vasić, Acetylcholinesterase inhibitors: pharmacology and toxicology, Curr. Neuropharmacol., 11 (2013) 315–35.
[7] G.F. Andrade, D.C.F. Soares, R.K. de Sousa Almeida, E.M.B. Sousa, Mesoporous silica SBA-16 functionalized with alkoxysilane groups: preparation, characterization, and release profile study, J. Nanomater., 75 (2012) 816496, doi: 10.1155/2012/816496.
[8] S. Chen, D. Sun, J.-S. Chung, Treatment of pesticide wastewater by moving-bed biofilm reactor combined with Fenton-coagulation pretreatment, J. Hazard. Mater., 144 (2007) 577–584.
[9] T.D. Lazarević-Pašti, A.M. Bondžić, I.A. Pašti, S.V. Mentus, V.M. Vasić, Electrochemical oxidation of diazinon in aqueous solutions *via* electrogenerated halogens – diazinon fate and implications for its detection, J. Electroanal. Chem., 692 (2013) 40–57.
[10] D. Farmanzadeh, H. Rezainejad, DFT study of adsorption of diazinon, hinosan, chlorpyrifos and parathion pesticides on the surface of $B_{36}N_{36}$ nanocage and its Fe doped derivatives as new adsorbents, Acta Phys. Chim. Sin., 32 (2016) 1191–1198.
[11] M. Cycoń, M. Wójcik, Z. Piotrowska-Seget, Biodegradation of the organophosphorus insecticide diazinon by *Serratia* sp. and *Pseudomonas* sp. and their use in bioremediation of contaminated soil, Chemosphere, 76 (2009) 494–501.
[12] J.G. Wu, C.Y. Lan, G.Y.S. Chan, Organophosphorus pesticide ozonation and formation of oxon intermediates, Chemosphere, 7 (2009) 1308–1314.
[13] J.G. Wu, L. Lin, T.G. Luan, Y.S.C. Gilbert, C.Y. Lan, Effects of organophosphorus pesticides and their ozonation byproducts on gap junctional intercellular communication in rat liver cell line, Food Chem. Toxicol., 45 (2007) 2057–2063.
[14] L. Yao, H. Yang, Z.S. Chen, M.Q. Qiu, B.W. Hu, X.X. Wang, Bismuth oxychloride-based materials for the removal of organic pollutants in wastewater, Chemosphere, 273 (2021) 128576, doi: 10.1016/j.chemosphere.2020.128576.
[15] R. Epsztein, O. Nir, O. Lahav, M. Green, Selective nitrate removal from groundwater using a hybrid nanofiltration–reverse osmosis filtration scheme, Chem. Eng. J., 279 (2015) 372–378.
[16] N. Singh, Adsorption of herbicides on coal fly ash from aqueous solutions, J. Hazard. Mater., 168 (2009) 233–237.
[17] N. Sivarajasekar, K. Balasubramani, N. Mohanraj, J. Prakash Maran, S. Sivamani, P. Ajmal Koya, V. Karthik, Fixed-bed adsorption of atrazine onto microwave irradiated *Aegle marmelos Correa* fruit shell: statistical optimization, process design and breakthrough modelling, J. Mol. Liq., 241 (2017b) 823–830.
[18] N. Sivarajasekar, N. Mohanraj, R. Baskar, S. Sivamani, Fixed-bed adsorption of ranitidine hydrochloride onto microwave assisted—activated *Aegle marmelos Correa* fruit shell: statistical optimization and breakthrough modelling, Arabian J. Sci. Eng., 43 (2017) 2205–2215.
[19] N. Sivarajasekar, T. Paramasivan, S. Muthusaravanan, P. Muthukumaran, S. Sivamani, Defluoridation of water using adsorbents – a concise review, J. Environ. Biotechnol. Res., 6 (2017) 186–198.
[20] T. Robinson, G. McMullan, R. Marchant, P. Nigam, Remediation of dyes in textile effluent: a critical review on current treatment technologies with a proposed alternative, Bioresour. Technol., 77 (2001) 247–255.
[21] M. Greluk, Z. Hubicki, Efficient removal of Acid Orange 7 dye from water using the strongly basic anion exchange resin Amberlite IRA-958, Desalination, 278 (2011) 219–226.
[22] U. Vijayalakshmi, A. Balamurugan, S. Rajeswari, Synthesis and characterization of porous silica gels for biomedical applications, Trends Biomater. Artif. Organs, 18 (2005) 101–105.
[23] M.J. Hao, M.Q. Qiu, H. Yang, B.W. Hu, X.X. Wang, Recent advances on preparation and environmental applications of MOF-derived carbons in catalysis, Sci. Total Environ., 760 (2021) 143333, doi: 10.1016/j.scitotenv.2020.143333.
[24] Q.H. Wu, G.Y. Zhao, C. Feng, C. Wang, Z. Wang, Preparation of a graphene-based magnetic nanocomposite for the extraction of carbamate pesticides from environmental water samples, J. Chromatogr. A, 1218 (2011) 7936–7942.
[25] Q. Liu, J.B. Shi, L. Zeng, T. Wang, Y. Cai, G. Jiang, Evaluation of graphene as an advantageous adsorbent for solid-phase extraction with chlorophenols as model analytes, J. Chromatogr. A, 1218 (2011) 197–204.

[26] H. Koolivand, A. Sharif, M. Razzaghi Kashani, M. Karimi, M. Koolivand Salooki, M.A. Semsarzadeh, Functionalized graphene oxide/polyimide nanocomposites as highly CO_2-selective membranes, J. Polym. Res., 21 (2014) 599, doi: 10.1007/s10965-014-0599-9.
[27] M. Keshvardoostchokami, P. Bigverdi, A. Zamani, A. Parizanganeh, F. Piri, Silver@ graphene oxide nanocomposite: synthesize and application in removal of imidacloprid from contaminated waters, Environ. Sci. Pollut. Res., 25 (2017) 6751–6761.
[28] P.K. Boruah, B. Sharma, N. Hussain, M.R. Das, Magnetically recoverable Fe_3O_4/graphene nanocomposite towards efficient removal of triazine pesticides from aqueous solution: investigation of the adsorption phenomenon and specific ion effect, Chemosphere, 168 (2017) 1058–1067.
[29] Y. Shi, L. Peng, Y. Ding, Y. Zhao, G.H. Yu, Nanostructured conductive polymers for advanced energy storage, Chem. Soc. Rev., 44 (2015) 6684–6696.
[30] A.J. Heeger, Semiconducting polymers: the third generation, Chem. Soc. Rev., 39 (2010) 2354–2371.
[31] C.P. Li, J. Wang, H. Guo, S.J. Ding, Low temperature synthesis of polyaniline-crystalline TiO_2-halloysite composite nanotubes with enhanced visible light photocatalytic activity, J. Colloid Interface Sci., 458 (2015) 1–13.
[32] I.E. Mejias Carpio, J.D. Mangadlao, H.N. Nguyen, R.C. Advincula, D.F. Rodrigues, Graphene oxide functionalized with ethylenediamine triacetic acid for heavy metal adsorption and anti-microbial applications, Carbon, 77 (2014) 289–301.
[33] X. Zhong, Z.P. Lu, W. Kiang, B.W. Hu, The magnetic covalent organic framework as a platform for high-performance extraction of Cr(VI) and bisphenol A from aqueous solution, J. Hazard. Mater., 393 (2020) 122353, doi: 10.1016/j.jhazmat.2020.122353.
[34] K. Jasuja, V. Berry, Implantation and growth of dendritic gold nanostructures on graphene derivatives: electrical property tailoring and Raman enhancement, ACS Nano, 3 (2009) 2358–2366.
[35] H.L. Wang, Q.L. Hao, X.J. Yang, L. Lude, X. Wang, Graphene oxide doped polyaniline for supercapacitors, Electrochem. Commun., 11 (2009) 1158–1161.
[36] N.A. Kumar, H.-J. Choi, Y.R. Shin, D.W. Chang, L.M. Dai, J.-B. Baek, Polyaniline-grafted reduced graphene oxide for efficient electrochemical supercapacitors, ACS Nano, 6 (2012) 1715–1723.
[37] Y.-C. Yong, X.-C. Dong, M.B. Chan-Park, H. Song, P. Chen, Macroporous and monolithic anode based on polyaniline hybridized three-dimensional graphene for high-performance microbial fuel cells, ACS Nano, 6 (2012) 2394–2400.
[38] E. Mohseni, M.R. Yaftian, H. Shayani-jam, A. Zamani, F. Piri, Molecularly imprinted poly(4,4′-methylenedianiline) as electrochemical sensor for determination of 1-benzothiophene, Synth. Met., 259 (2020) 116252, doi: 10.1016/j.synthmet.2019.116252.
[39] N. Cai, P. Larese-Casanova, Application of positively-charged ethylenediamine-functionalized graphene for the sorption of anionic organic contaminants from water, J. Environ. Chem. Eng., 4 (2016) 2941–2951.
[40] N. Tahir, H.N. Bhatti, M. Iqbal, S. Noreen, Biopolymers composites with peanut hull waste biomass and application for Crystal Violet adsorption, Int. J. Biol. Macromol., 94 (2017) 210–220.
[41] M. Mushtaq, H.N. Bhatti, M. Iqbal, S. Noreen, *Eriobotrya japonica* seed biocomposite efficiency for copper adsorption: isotherms, kinetics, thermodynamic and desorption studies, J. Environ. Manage., 176 (2016) 21–33.
[42] K.-L. Chang, J.-H. Lin, S.-T. Chen, Adsorption studies on the removal of pesticides (Carbofuran) using activated carbon from rice straw agricultural waste, World Acad. Sci. Eng. Technol., 5 (2011) 4–21.
[43] A. Chham, E. Khouya, M. Oumam, A.K. Abourriche, S. Gmouh, M. Larzek, S. Mansouri, N. Elhammoudi, N. Hanafi, H. Hannache, The use of insoluble mater of Moroccan oil shale for removal of dyes from aqueous solution, Chem. Int., 4 (2018) 67–76.
[44] N.E. Fairooz, Z.A. Jwad, M.A.A. Zahra, Adsorption isotherms and thermodynamic data for removal pesticides from aqueous solution on pomegranate peel surface, Am. J. Appl. Chem., 3 (2015) 147–152.
[45] S. Liang, X.Y. Guo, N.C. Feng, Q.H. Tian, Isotherms, kinetics and thermodynamic studies of adsorption of Cu^{2+} from aqueous solutions by Mg^{2+}/K^+ type orange peel adsorbents, J. Hazard. Mater., 174 (2010) 756–762.
[46] D.J. Ju, I.G. Byun, J.J. Park, C.H. Lee, G.H. Ahn, T.J. Park, Biosorption of a reactive dye (Rhodamine-B) from an aqueous solution using dried biomass of activated sludge, Bioresour. Technol., 99 (2008) 7971–7975.
[47] H. Freundlich, A. Seal, Ueber einige Eigenschaften des Rhodanions. Colloids Polym. Sci., 11 (1912) 257–263.[48]I . Langmuir, J. Am. Chem. Soc., 40 (1918) 1361–1403.
[48] I. Langmuir, The adsorption of gases on plane surfaces of glass, mica and platinum, J. Am. Chem. Soc., 40 (1918) 1361–1403.